Polariton states in disordered organic microcavities

P. Michetti and G. C. La Rocca
Scuola Normale Superiore and INFM, Piazza dei Cavalieri 7, I-56126 Pisa, Italy
(Received 15 November 2004; published 22 March 2005)

In typical organic based microcavities, large values of Rabi splitting are accompanied by any amount of structural disorder. We present a microscopic approach which treats on equal footing the strong light-matter coupling and the disorder scattering which breaks translational symmetry. Through direct numerical diagonalization in a long, but finite, disordered one-dimensional microcavity, the nature of the eigenstates is elucidated and compared to that of the plane-wave-like cavity polaritons of a perfect system. It is shown that delocalized states with well defined wave vectors or strongly localized states may occur, depending on their energy. In particular, at energies close to the excitonic resonance as well as at the bottom of the polariton branches, the states are definitely not plane-wave-like.

DOI: 10.1103/PhysRevB.71.115320 PACS number(s): 78.66.Qn, 78.40.Me, 71.36.+c, 71.35.Cc

I. INTRODUCTION

Inorganic semiconductor microcavities in the strong coupling regime, in which a confined photon mode is hybridized with a resonant electronic excitation, e.g., a quantum well Wannier-Mott exciton, giving rise to two cavity polariton states separated by the Rabi splitting, have been intensively studied as they exhibit many novel linear and nonlinear optical properties.[1] Recently, organic based microcavities having much larger Rabi splitting values, typically of the order of 100 meV or more, have for this reason attracted a lot of attention.[2] While the photonic component of such systems is quite similar to that of inorganic based microcavities, their optically active electronic resonances are quite different being molecular excitations rather than large radius excitons. In particular, due to electron-phonon interaction or disorder scattering the molecular Frenkel excitons may behave as incoherent (diffusive) excitations rather than Bloch plane waves having a well defined wave vector and group velocity.[3]

In organic microcavities, the strong light-matter coupling giving rise to plane-wave-like cavity polariton states is favored by the large oscillator strength of Frenkel excitons.[4] However, as their optically active layer is not crystalline, typical organic microcavities are also disordered to a high degree. Thus, in the strong coupling regime, on the one hand the light-matter interaction induces the formation of delocalized polariton states with a well defined wave vector, on the other hand the structural disorder which scatters the excitons and breaks the translational invariance brings about localized states quite different from plane-wave-like polaritons.

Close to the exciton energy, in particular, a significant density of incoherent states may remain present, as also evident from the observation of a third luminescence peak,[2,5] the energy of which does not depend on the angle of observation, between the upper (UP) and lower (LP) polariton ones which follow instead the usual cavity polariton dispersion. A macroscopic approach,[6] briefly discussed below in Sec. II to introduce all relevant definitions, predicts how the traditional picture of coherent plane-wave-like cavity polaritons breaks down at the bottom of both polariton branches and for the LP branch where it flattens approaching the bare exciton resonance.

It is our purpose in the present work to develop a microscopic approach treating both the light-matter coupling and the disorder scattering on equal footing in order to elucidate the character of the resulting cavity eigenstates and to substantiate the macroscopic picture. The microscopic model is introduced in Sec. III, while the results of the numerical simulations are presented and discussed in Sec. IV; finally, conclusions are drawn.

II. MACROSCOPIC APPROACH

In the macroscopic approach,[6] the cavity polariton modes are directly obtained from the solution of Maxwell's equations with the complex dielectric function appropriate for an excitonic resonance and boundary conditions determined by the cavity mirrors. Assuming for the sake of simplicity perfect mirror boundary conditions, the confined photon mode dispersion in an "empty" microcavity of width L_c as a function of the in-plane wave vector q is

$$E_{cav}(q) = \frac{\hbar c}{\sqrt{\varepsilon_b}} \sqrt{\frac{\pi^2}{L_c^2} + q^2}, \tag{1}$$

where ε_b is the background dielectric constant. The dielectric function including the resonant contribution is given by

$$\varepsilon(\omega) = \varepsilon_b + \frac{A}{E_0^2 - (\hbar\omega)^2 - 2i\hbar\omega\gamma_0}, \tag{2}$$

where E_0 is the dispersionless exciton energy, γ_0 is the total (homogeneous plus inhomogeneous) broadening of the excitonic resonance, and the constant A is proportional to the oscillator strength of the transition. Then, from Maxwell's equations follows

$$\hbar^2 c^2 (q^2 + \pi^2/L_c^2) = \varepsilon(\omega)(\hbar\omega)^2, \tag{3}$$

and the cavity polariton modes near resonance **($\hbar\omega \approx E_{cav}(q) \approx E_0$)** are obtained as the solutions of

$$[\hbar\omega - E_{cav}(q)](\hbar\omega - E_0 + i\gamma_0) = (\Omega/2)^2, \tag{4}$$

where $\Omega = \sqrt{A/\varepsilon_b}$ is the Rabi splitting.[7]

The solution of Maxwell's equations with a complex dielectric function leads in general to both a complex frequency $\omega=\omega'+i\omega''$ and a complex wave vector $q=q'+iq''$, i.e., to modes having an uncertainty both in energy and wave vector. Assuming the dissipation to be small ($\gamma_0<\Omega$) and taking a real wave vector, from Eq. (4) the following cavity polariton dispersion curves and energy broadenings are obtained:

$$E_{U,L}(q)=\frac{E_{cav}(q)+E_0}{2}\pm\frac{1}{2}\sqrt{\Omega^2+[E_{cav}(q)-E_0]^2}, \quad (5)$$

$$\Delta E_{U,L}(q)=\gamma_0|c_{ex}^{(U,L)}(q)|^2=\frac{\gamma_0\Omega^2}{\Omega^2+4[E_0-E_{U,L}(q)]^2}, \quad (6)$$

where $|c_{ex}^{(U,L)}|^2$ are the exciton weights in the polaritonic states. However, semiclassical wave-packets with a well defined wave vector and energy will be rather characterized as having both an energy uncertainty ΔE and a wave vector uncertainty Δq, *provided* that $\Delta E \ll E$ *and* $\Delta q \ll q$. Such cavity polariton quasiparticles will be coherent states moving with a group velocity $v_g=\partial\omega/\partial q$ as obtained from Eq. (5). Correspondingly, the wave vector uncertainty can be estimated as $\Delta q=\Delta E/(\hbar v_g)$ and from the equations above,

$$\Delta q_{U,L}(q)=\frac{\gamma_0\varepsilon_b E_{cav}(q)}{c^2\hbar^2 q}\frac{4[E_{cav}(q)-E_{U,L}(q)]^2}{\Omega^2}. \quad (7)$$

Therefore, for cavity polaritons it is clear that while the condition $\Delta E \ll E$ is not restrictive, the condition $\Delta q \ll q$ breaks down (i) for $q\to 0$ for both branches and (ii) for large q for the lower polariton branch. The points along the dispersion branches where $\Delta q=q$ can be taken as the "end points" restricting the spectral and wave vector range where plane-wave-like cavity polariton states may exist.[6] It is to be noted that while in case (ii) above the eigenstates can be considered to be incoherent exciton states not affected by the strong coupling, in case (i) the states are still hybrid states with a significant cavity photon-exciton coupling for which, however, the wave vector is not a good quantum number.

III. MICROSCOPIC 1D MODEL

We notice that even though the cavity polariton quasiparticles considered above are expected to be localized over a distance of the order of $1/\Delta q$, the macroscopic approach does not explicitly introduce any translational symmetry breaking effect. In particular, it does not allow to assess the character of the wave functions when they are no longer plane-wave-like and it can only take the disorder into account in an effective phenomenological way through the energy broadening of the exciton resonance. The microscopic model presented in the following does not have such shortcomings. However, for reasons of numerical complexity, it must be limited to the one-dimensional case (rather than a planar two-dimensional one). This limitation is not expected to change in any significant way the physics of the interplay between the light-matter strong coupling and the translational symmetry breaking disorder scattering, just as in the case of inorganic microcavities.[8]

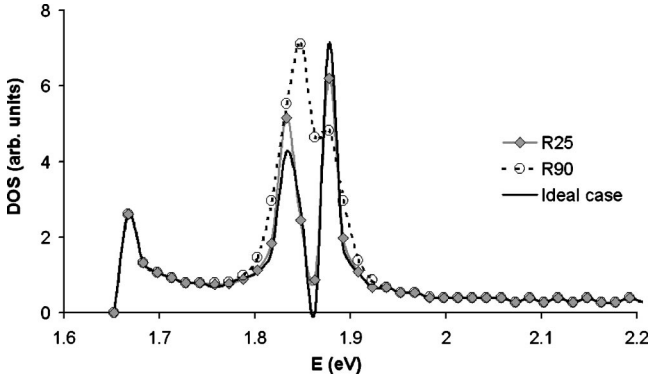

FIG. 1. Density of states (in arbitrary units) for diagonal energy disorder of different strength: the diamonds correspond to $\gamma_0=25$ meV, the circles to $\gamma_0=90$ meV (the solid line is the result with no disorder).

The microscopic model is set up in the simplest possible way to address the competition of the strong light-matter coupling with the localization effects due to structural disorder, neglecting all other inessential features. The one-dimensional microcavity is considered to be a rectangular waveguide with perfectly reflecting walls of sides $L_y<L_x$ in which a confined photon mode polarized along y propagates along the z axis with wave vector q and dispersion given by Eq. (1) with $L_c=L_x$. In the ideal case without disorder, the optically active material is modeled by a 1D lattice of independent two-level molecules along the axis of the one-dimensional microcavity, each one having a resonance of energy E_0 and transition dipole matrix element $\vec{P}=P_0\hat{y}$. No direct interaction among the molecules is included, i.e., in the absence of the coupling with the photon mode an electronic excitation is localized on a single molecule. No dissipation is included, i.e., perfect mirrors are assumed and the lifetime of electronic excitations is supposed infinite.

Static structural disorder of different kinds is taken into account as follows. Diagonal energy disorder is included writing the resonant energy of molecule j as $E_j=E_0+\delta E_j$, δE_j being a stocastic variable Gaussian distributed with zero mean and a width corresponding to the exciton linewidth γ_0 (i.e., the value of γ_0 gives the strength of the on-site energy disorder). Positional disorder is included assuming that the position of molecule j along z is $z_j=ja+\delta z_j$, where a is the 1D lattice constant and δz_j a stocastic variable Gaussian distributed with zero mean and a width which is a fraction of a. Orientational disorder is included writing the projection of the transition dipole moment of molecule j along the polarization of the photon mode as $\vec{P}_j\cdot\hat{y}=P_0\eta_j$ with $-1\leqslant\eta_j\leqslant 1$ a stocastic variable the distribution of which peaks at the value of unit with an average value $\overline{\eta}$ which is a fraction of unit (i.e., increasing orientational disorder corresponds to lower values of $\overline{\eta}$, the distribution shape being that of a half Gaussian).

The model Hamiltonian comprises two diagonal blocks (the first referring to the electronic excitations labeled by their site index j, the second to the one-dimensional cavity photon modes labeled by their wave vector q) with an off-diagonal coupling due to the light-matter interaction given by

$$H_{j,q} \propto \frac{E_j P_0 \eta_j}{\sqrt{L_x L_y L_z \varepsilon_b E_{cav}(q)}} \exp(iqz_j), \tag{8}$$

where L_z is the length of a long quantization box along the z axis. In the above, it has been assumed that the modulus of the transition dipole moment P_0 is constant and that the x coordinate of all molecules is fixed at the antinode of the cavity photon mode. These are not crucial restrictions as the effects of their variations can be considered to be included in the "orientational" stocastic variable η_j. The latter is the disorder contribution which has the strongest effect when η_j takes both positive and negative values. On the contrary, the effects of positional disorder are rather weak simply because $q\,\delta z_j \ll 1$, and they will not be considered in detail. Finally, the effects of the on-site energy disorder (appearing in the diagonal electronic excitation block) can be very significant.

In the next section, the results of a direct numerical diagonalization of the Hamiltonian of the disordered system will be presented and discussed. For each disorder configuration all eigenstates and eigenvectors are found and analyzed, then configurational averages of significant physical quantities are calculated.

IV. NUMERICAL RESULTS AND DISCUSSION

In order to solve numerically the microscopic model above, the parameters of the corresponding ideal system without disorder have been chosen as follows. To be definite, the most common case of a negatively detuned cavity has been considered with $E_{cav}(q=0)=1.69$ eV and $E_0=1.85$ eV, and the P_0 value chosen to have a Rabi splitting $\Omega=120$ meV, typical for organic microcavities. To limit the calculation load without affecting the physics of the problem, the basis used is of $N=488$ molecule sites ($|ex,j\rangle$) spaced by $a=150$ nm along the length of the cavity ($L_z=Na=73$ μm) and 295 photon modes ($|ph,q\rangle$) equally spaced at wave vector intervals of $2\pi/L_z=860$ cm^{-1} and covering the lowest one-dimensional cavity mode from its cutoff up to an energy of about 2.3 eV, value at which the coupling with the electronic excitations is already negligible. We notice that the size of the Brillouin zone of the lattice of molecules $\pi/a \simeq 2.1\times10^5$ cm^{-1} is significantly larger than the maximum photon mode wave vector considered $q_{max}\simeq 1.3\times10^5$ cm^{-1}. Thus, even in the ideal case in our numerical simulations a large number of electronic excitations (about 40%) remain uncoupled. This is, however, quite acceptable as in reality they would correspond to lower polaritons having large wave vectors and a nearly negligible photon component. To be consistent, in the presence of disorder, only eigenstates having a photon component of at least 2% have been included in the analysis. Other states are within our numerical simulation not coupled to light, and thus correspond, with or without disorder, to purely molecular excitations with an energy close to the bare exciton energy E_0.

For a given disorder realization, all eigenstates and eigenvalues are calculated. The eigenstates are expressed in our basis as follows:

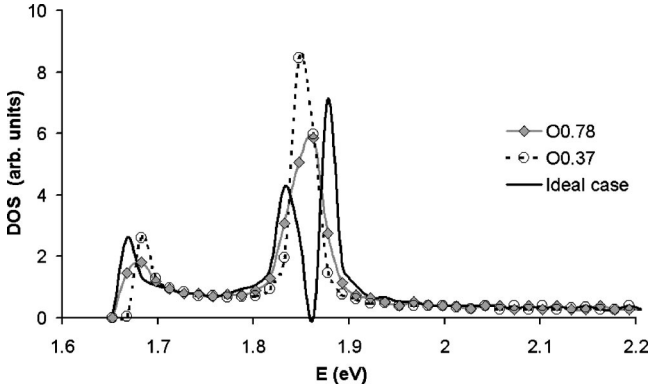

FIG. 2. Density of states (in arbitrary units) for orientational disorder of different strength: the diamonds correspond to $\overline{\eta}=0.78$, the circles to $\overline{\eta}=0.37$ (the solid line is the result with no disorder).

$$|\psi\rangle = \sum_j c_{ex}(j)|ex,j\rangle + \sum_q c_{ph}(q)|ph,q\rangle. \tag{9}$$

Excluding those corresponding to purely molecular excitations as mentioned above, the wave functions are analyzed to extract quantities relevant to characterize their degree of localization. The analysis can be done for the excitonic component in real space using $c_{ex}(j)$ and for the photonic component in wave vector space using $c_{ph}(q)$, or *vice versa* by the respective Fourier transforms. In particular, we calculate the exciton inverse participation rate (**I_{ex}**

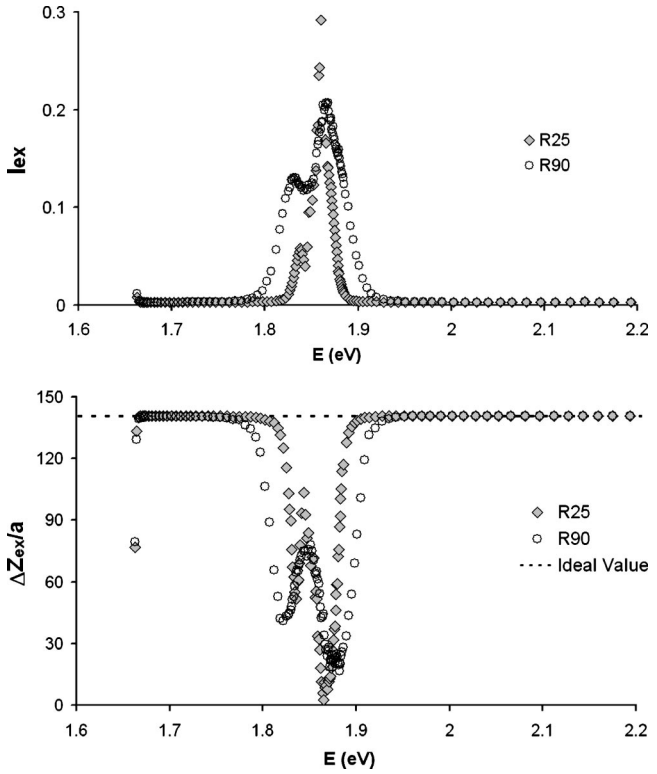

FIG. 3. Inverse participation ratio (top) and mean position standard deviation (bottom, in units of lattice constant) of the exciton component for diagonal energy disorder of different strength: the diamonds correspond to $\gamma_0=25$ meV, the circles to $\gamma_0=90$ meV.

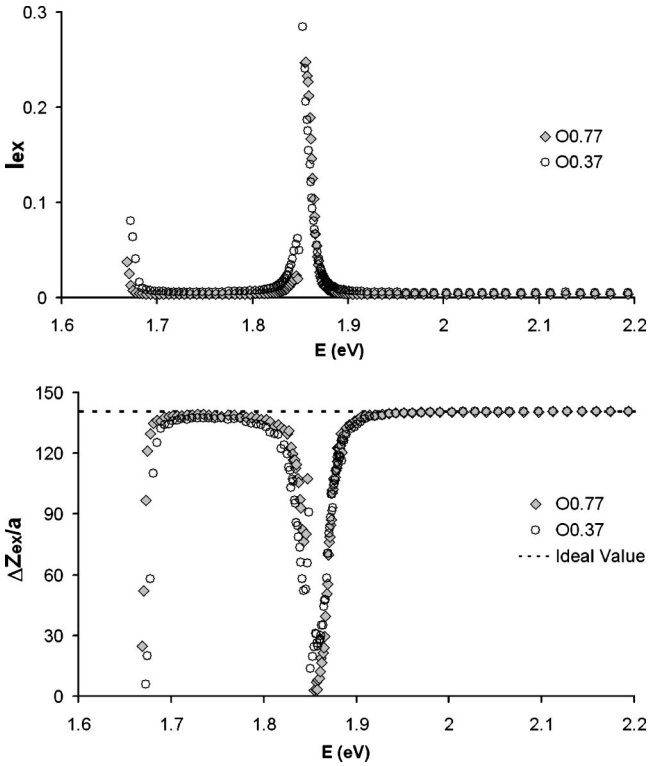

FIG. 4. Inverse participation ratio (top) and mean position standard deviation (bottom, in units of lattice constant) of the exciton component for orientational disorder of a different strength: the diamonds correspond to $\overline{\eta}=0.78$, the circles to $\overline{\eta}=0.37$.

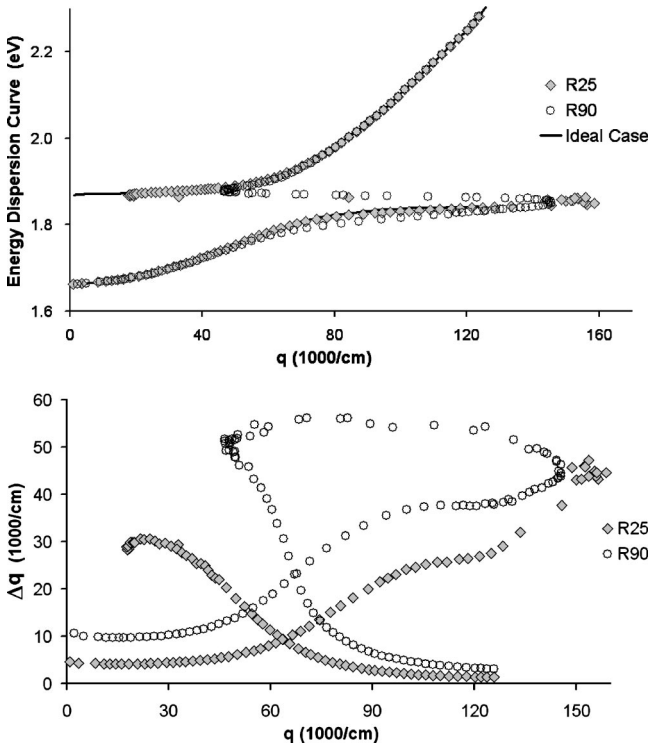

FIG. 5. Energy dispersion curve obtained from the mean wave vector $\overline{q}$ of the excitonic component (top) and its standard deviation Δq (bottom) for a diagonal energy disorder of a different strength: the diamonds correspond to $\gamma_0=25$ meV, the circles to $\gamma_0=90$ meV.

$=\Sigma_j|c_{ex}(j)|^4/[\Sigma_j|c_{ex}(j)|^2]^2$**)** and the mean position standard deviation Δz_{ex}, and the corresponding quantities for the photonic component from the Fourier transform of $c_{ph}(q)$. In addition, to reconstruct the dispersion relations, we calculate the mean value of the wave vector $\overline{q}$ and its standard deviation Δq from $c_{ph}(q)$ or from the Fourier transform of $c_{ex}(j)$, respectively, for the photonic and excitonic components. For each eigenstate of the disordered system, we also determine the ideal cavity polariton (ICP) state which has the highest overlap with it. The latter quantity is here introduced as a very effective measure of the global effect of disorder on the system eigenstates. The numerical results presented in the figures and discussed below, a part from a few examples of specific individual eigenfunctions, have been obtained after configurational averaging. All calculations have been repeated for about 500 disorder realizations and averaged summing over the eigenstates within 150 small spectral intervals in which the entire spectrum is subdivided. The width of these small spectral intervals is chosen in such a way that each of them for a given disorder realization typically contains about 5 eigenvalues.

The effects of disorder of increasing strength on the density of states (DOS) are shown in Figs. 1 and 2 for diagonal energy disorder and orientational disorder, respectively. For comparison, the solid line shows the corresponding DOS with no disorder, in which case the square root singularities typical of one-dimensional systems are smoothed by finite size effects in our numerical simulations. In both figures, it is evident a build-up of DOS at energies close to the bare exciton energy between the UP and LP branches. For the case of orientational disorder, the two DOS peaks corresponding to the lower edge of the UP branch and the upper edge of the LP branch are no longer resolved. Furthermore, orientational disorder also affects the bottom of the lower polariton (LP) branch. In general, disorder effects are less important in the spectral regions far from the edges of the ideal cavity polariton dispersion branches.

Figures 3 and 4 show the localization properties of the excitonic component for diagonal energy disorder and orientational disorder, respectively, as measured by the inverse participation ratio I_{ex} and by the mean position standard deviation Δz_{ex}. The inverse participation ratio would be of order 1 for a completely localized state and of order $1/N=1/488$ for a completely delocalized one, while the standard deviation of the mean position is of the order of the localization radius and, for our sample of 488 sites, would be about $140a$ for a completely delocalized state. In both Fig. 3 and Fig. 4, the localization effects of disorder are evident and affect particularly the spectral region near the bare exciton energy and, more markedly for orientational disorder, the bottom of the LP branch. In these spectral regions I_{ex} grows, whereas Δz_{ex} correspondingly decreases down to values of only a few lattice spacings. Analogous information is obtained from an analysis of the photonic component of the disordered eigenstates.

In Fig. 5, we show the dispersion relation of the system with diagonal energy disorder obtained from the calculation of the mean value $\overline{q}$ of the wave vector of the excitonic

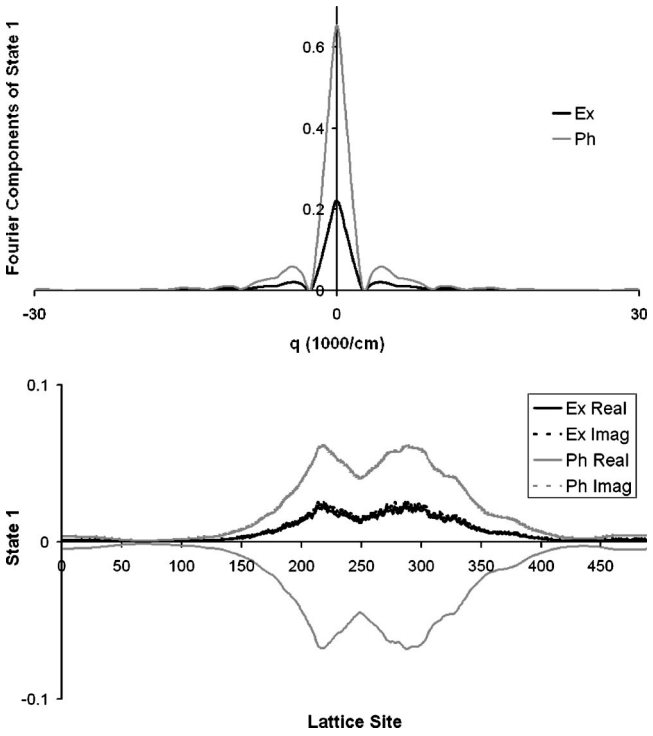

FIG. 6. Eigenfunction corresponding to the bottom of the LP branch ($E=1.663$ eV) in Fourier space (top) and in real space (bottom).

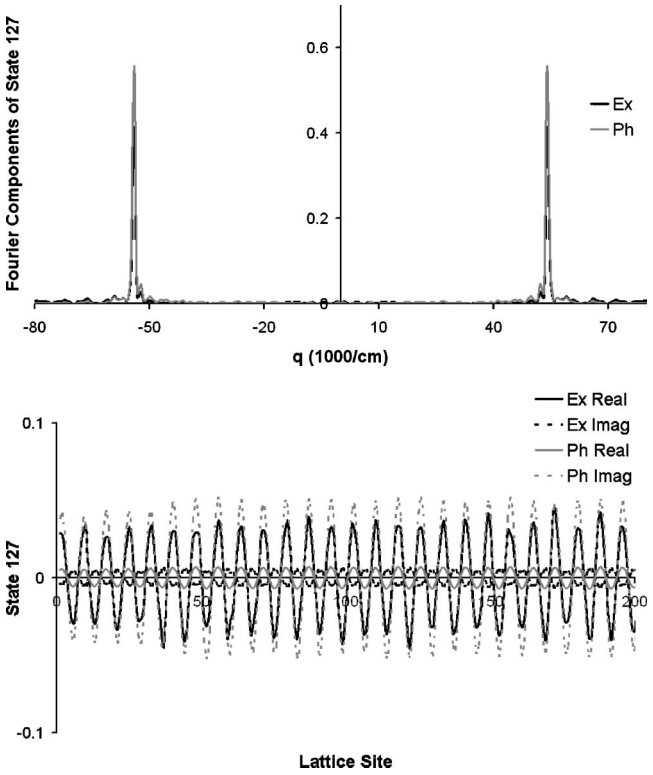

FIG. 7. Eigenfunction corresponding to the middle of the LP branch ($E=1.767$ eV) in Fourier space (top) and in real space (bottom).

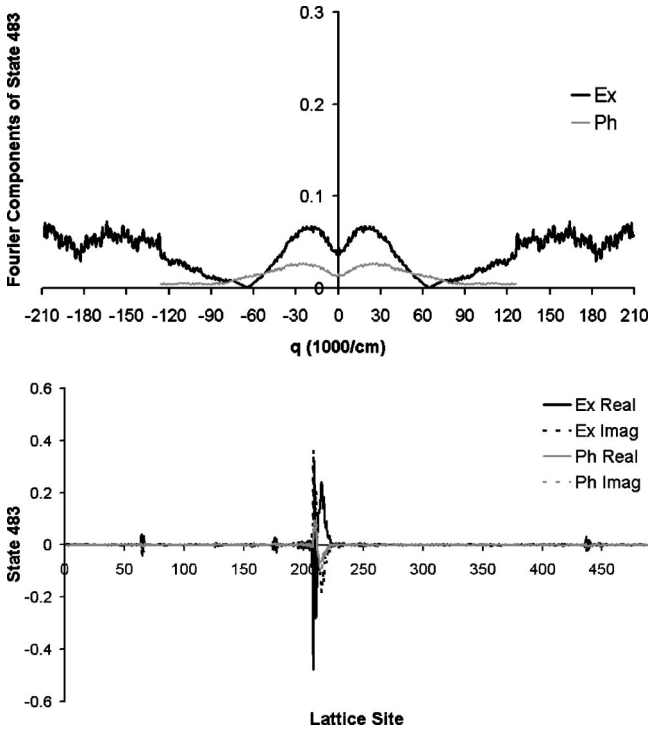

FIG. 8. Eigenfunction corresponding to the spectral range between the UP and the LP branches ($E=1.863$ eV) in Fourier space (top) and in real space (bottom).

component of the eigenstates: it is noticeable that the spectral region between UP and LP branches where there is little dispersion corresponding to localized states with an ill defined wave vector, i.e., a large Δq. Similar information is obtained from the corresponding analysis of the photonic component, while in the case of orientational disorder the wave vector of the excitonic component is even less defined.

As illustrative examples of the different character of the eigenstates, a few specific wave functions are shown in Figs. 6–8 for the case of diagonal energy disorder with $\gamma_0 = 50$ meV. The state in Fig. 6 is representative of the few states at the bottom of the LP branch with a localized character, in this case with $\Delta z_{ex} \simeq 70a$. Notice also the rather broad peak in its Fourier transform around $q=0$. Yet, this

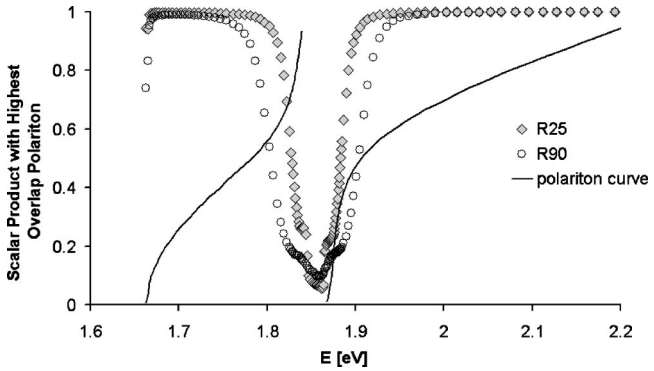

FIG. 9. Highest overlap with ideal cavity polariton (ICP) states for the diagonal energy disorder of different strength: the diamonds correspond to $\gamma_0=25$ meV, the circles to $\gamma_0=90$ meV (the solid line is the ICP dispersion relation).

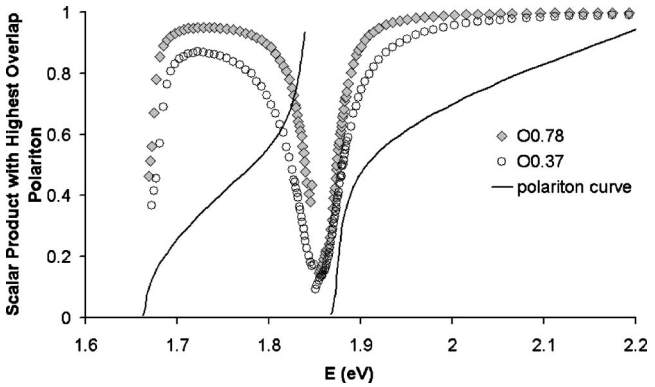

FIG. 10. Highest overlap with ideal cavity polariton (ICP) states for an orientational disorder of a different strength: the diamonds correspond to $\overline{\eta}=0.78$, the circles to $\overline{\eta}=0.37$ (the solid line is the ICP dispersion relation).

state is still a hybrid of excitonic and photonic components, the excitonic weight being about 10%. The state in Fig. 7 is in the middle of the LP branch and has a plane-wave-like character similar to an ideal cavity polariton (ICP) state. Its Fourier spectrum is dominated by two strong and narrow peaks at $\pm q \simeq 5.5\times 10^4$ cm^{-1}. The state in Fig. 8 is from the dispersionless spectral region between UP and LP branches and has a strongly localized character with a highly fragmented structure and a rather small photon component of about 7%. Its Fourier spectrum is correspondingly structureless.

As mentioned above, the highest overlap of a disordered eigenfunction with an ideal cavity polariton state (ICP) can be taken as a figure of merit of the quality of the system: the lower this quantity is, the stronger the localization effects of disorder are in the corresponding spectral region. For instance, for the state shown in Fig. 8 it is less than 0.1, while for the one in Fig. 7 it is 0.98. The behavior of the highest overlap with an ICP as a function of energy is shown in Figs. 9 and 10 for diagonal energy disorder and orientational disorder, respectively, confirming that the localization is stronger at energies near the bare exciton energy and at the bottom of the LP branch, with a more pronounced effect of orientational disorder.

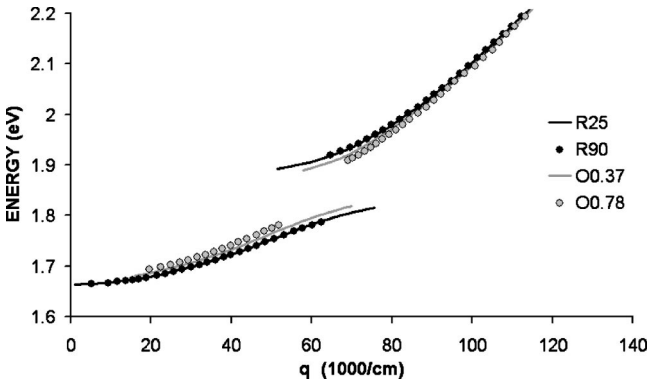

FIG. 11. Dispersion curves of well defined quasiparticles: the black solid line and the black circles indicate the plane-wave-like cavity polaritons in the presence of an energy diagonal disorder for, respectively, $\gamma_0=25$ meV and $\gamma_0=90$ meV; the gray solid line and the gray circles indicate the plane-wave-like cavity polaritons in the presence of orientational disorder for, respectively, $\overline{\eta}=0.78$ and $\overline{\eta}=0.37$. In all cases, the upper branch can be indefinitely extended to higher energies.

TABLE I. Wave vector end points (in units of 1000 cm^{-1}) of the plane-wave-like quasiparticle dispersion branches for two values of diagonal disorder compared to the corresponding predictions of the macroscopic approach.

	k_{min}^{LP}	k_{max}^{LP}	k_{min}^{UP}	k_{min}^{LP} mac.	k_{max}^{LP} mac.	k_{min}^{UP} mac.
$\gamma_0=50$ meV	1.1	69	62	7.7	95	45
$\gamma_0=90$ meV	5.0	62	65	10	83	50

In the macroscopic model discussed above, the condition defining the extension of the plane-wave-like cavity polariton dispersion curves is $\Delta q \leqslant q$. As we have detailed information on the actual eigenfunction $|\psi\rangle$ in the presence of the microscopic disorder, we will use the following heuristic condition based on the value of the highest ICP overlap: $|\langle \mathrm{ICP}|\psi\rangle| \geqslant 0.8$. The corresponding "end points" of the plane-wave-like cavity polariton dispersion curves can be read from Fig. 11 for the diagonal energy disorder or the orientational disorder. For increasing disorder strength, the plane-wave-like regions schrink. The microscopic criterion here used gives results in good agreement with those of the macroscopic approach,[6] as shown in Table I for a few examples, considering that in both the microscopic and macroscopic treatments the "end points" are not sharply defined as the transition between incoherent (localized) states and coherent (plane-wave-like) quasiparticles is a smooth one.

V. CONCLUSIONS

In this work, we have used a microscopic approach to describe the effects of disorder on the polariton states of an organic microcavity. The competition between the translational symmetry breaking scattering and the strong light-matter coupling leads to the coexistence of states with different character in various spectral regions. Not only close to the bare exciton energy the states are localized, but also at the bottom of the LP branch they no longer have a well defined wave vector, though they are still strongly coupled with light. These microscopic results substantiate the predictions of a macroscopic model and provide a complete description of the eigenfunctions of the system. The approach developed here will allow us to calculate microscopically other quantities, such as the matrix elements of the electron-phonon interaction in the presence of a disorder, which are needed for a detailed description of the behavior of cavity polaritons in organic microcavities.

ACKNOWLEDGMENTS

It is a pleasure to thank Vladimir Agranovich and Franco Bassani for many stimulating discussions. Partial financial support from the EC (HYTEC contract HPRN-CT-2002-00315) is gratefully acknowledged.

[1] For a review see M. S. Skolnick, T. A. Fisher, and D. M. Whittaker, Semicond. Sci. Technol. **13**, 645 (1998); G. Khitrova, H. M. Gibbs, F. Jahnke, M. Kira, and S. W. Koch, Rev. Mod. Phys. **71**, 1591 (1999); A. Kavokin and G. Malpuech, *Cavity Polaritons*, *Thin Films and Nanostructures* (Elsevier, New York, 2003), Vol. 32; C. Ciuti, P. Schwendimann, and A. Quattropani, Semicond. Sci. Technol. **18**, S279 (2003).

[2] For a review see D. G. Lidzey, in *Organic Nanostructures: Science and Applications*, edited by V. M. Agranovich and G. C. La Rocca (SIF, IOS Press, Amsterdam, 2002), p. 405; D. G. Lidzey, Chap. 8 in *Thin Films and Nanostructures*, edited by V. M. Agranovich and F. Bassani (Elsevier, New York, 2003), Vol. 31, Chap. 8.

[3] M. D. Fayer, in *Spectroscopy and Excitation Dynamics of Condensed Molecular Systems*, edited by V. M. Agranovich and R. M. Hochstrasser (North-Holland, Amsterdam, 1983), p. 185.

[4] V. M. Agranovich, H. Benisty, and C. Weisbuch, Solid State Commun. **102**, 631 (1997).

[5] D. G. Lidzey, A. M. Fox, M. D. Rahn, M. S. Skolnick, V. M. Agranovich, and S. Walker, Phys. Rev. B **65**, 195312 (2002).

[6] V. M. Agranovich, M. Litinskaia, and D. G. Lidzey, Phys. Rev. B **67**, 085311 (2003).

[7] V. Savona, L. C. Andreani, P. Schwendimann, and A. Quattropani, Solid State Commun. **93**, 733 (1995).

[8] V. Savona, C. Piermarocchi, A. Quattropani, F. Tassone, and P. Schwendimann, Phys. Rev. Lett. **78**, 4470 (1997); D. M. Whittaker, *ibid.* **80**, 4791 (1998).